INDIAN JOURNAL OF SCIENCE AND TECHNOLOGY

ORIGINAL ARTICLE

Ruthenium (III)-Catalyzed Chloramphenicol's Degradation by Peroxymonosulfate in Basic Medium: A Kinetic and Computational Investigation

Anita Meena[1], **Dilip Kumar**[1]*

1 Kinetics Laboratory, Department of Chemistry, Faculty of Science, Jai Narain Vyas University, New Campus, NH- 65 Jodhpur, Rajasthan, 342001, INDIA

OPEN ACCESS

Received: 26/01/2026

Accepted: 06/02/2026

Published: 21/02/2026

Citation: Meena A, Kumar D (2026) Ruthenium (III)-Catalyzed Chloramphenicol's Degradation by Peroxymonosulfate in Basic Medium: A Kinetic and Computational Investigation. Indian Journal of Science and Technology 19(6): 355-367. https://doi.org/10.17485/IJST/v19i6.100

* **Corresponding author**.

dilipkumar.m2103@gmail.com

Funding: None

Competing Interests: None

Published By Indian Society for Education and Environment (iSee)

ISSN
Print: 0974-6846
Electronic: 0974-5645

Abstract

Objectives: This study presents Ruthenium catalysed degradation of Chloramphenicol by peroxymonosulphate (PMS) in basic medium. **Method**: This study tests a range of results in basic solutions. Experiments were conducted with varying kinetic and thermodynamic variables. To investigate the oxidation of chloramphenicol we applied the common titrimetric analysis. The rate of oxidation of chloramphenicol was evaluated by using titrimetric analysis in which the amount of oxidant remaining unreacted in reaction mixture were measured at regular time intervals using iodometric method. To calculate and corelate the results, the DFT parameters are used. **Findings:** This work introduces a mechanistically resolved kinetic framework for the Ru (III)-catalysed oxidation of chloramphenicol by peroxymonosulphate in alkaline solution. Unlike many substrate-focused oxidation studies, the kinetic signatures here identify oxidant activation as the dominant control element. The rate is first order in PMS and Ruthenium (III) with a finite intercept, cleanly separating catalytic turnover from a parallel uncatalyzed pathway. The weak/saturation-type dependence on chloramphenicol identifies oxidant activation (Ru–PMS) as the turnover-limiting step rather than substrate oxidation. Strong hydroxide inhibition and a pronounced inverse ionic-strength effect ($KCl/NaClO_4$) diagnose speciation- and electrostatics-controlled formation of the activated complex, enabling a composite rate law with physical-organic significance. We also determined the thermodynamic functions and Eyring activation parameters for the rate-determining (slow) step, thereby providing an energetic basis for the proposed mechanism. In addition, density functional theory (DFT) calculations were performed to characterize the electronic structure and optimized geometry of chloramphenicol and peroxymonosulphate. **Novelty:** The combined kinetic–thermodynamic analysis and DFT modeling therefore offer a coherent experimental–computational description of the Ru(III)–PMS oxidation pathway in alkaline medium

Keywords: Chloramphenicol; Kinetic investigation; Oxidation; Chloramphenicol; peroxymonosulphate; Ruthenium (III); Basic Medium

1 Introduction

Kinetic and thermodynamic investigation of Chloramphenicol (CAP) in the basic medium is a special key to scientific progress. Chloramphenicol are compounds composed of metal and oxygen elements. Chloramphenicol (CAP) is an anti ribosomal antibiotic [1] and first quarantined from the bacteria Streptomyces venezuelae in 1947 [2]. Kaur et al., studied on rapid detection and visible light driven photocatalytic degradation of chloramphenicol in aqueous medium using a $CoAl_2O_4$/Rgo nanocomposite [3]. Singh reported on Osmium (VIII)- catalyzed oxidative degradation of paracetamol by chloramine-T in an aqueous alkaline medium: computational screening and mechanistic pathways [4]. Arpitha et al., studied comparative kinetic study of uncatalyzed and Ce(IV) catalyzed cetirizine dihydrochloride oxidation in aqueous acid medium by chloramine-T [5]. Among these techniques, thermal decomposition is one of the most used methods, which involves heating the metal salt solution or metal compound to high temperatures to decompose and generate metal oxides. Metal oxides have a wide range of applications. Many scientists studied the degradation of chloramphenicol by using different metallic and non-metallic oxidants in aqueous solutions by incorporating different approaches. Byadagi et al. examined the degradation of the drug chloramphenicol (CAP) by Cu (III) in the presence of Pd(II) and Os(VIII) catalysts [6]. Zhang et al. researched on chlorination and photocatalytic degradation of chloramphenicol [7]. Zhou et al. reported on potassium ferrate (VI), direct UV irradiation, persulfate (PS) oxidation [8]. Tan et al. worked on irradiation-activated persulfate process [9]. According to Cheng et al., graphene oxide (GO) has amazing reactivity, enhancing the Fe (III)/H_2O_2 performance for CAP degradation [10]. According to Shmychkova et al., the cleavage of dichloroacetic acid produces 4-(-2-amino-1,3-dihydroxy-propanyl)-nitrobenzene by the electrochemical oxidation of chloramphenicol with lead dioxide [11]. In [12], investigated the kinetics of isothermal torrefaction of sorghum distilled residue (SDR), the main byproduct of the sorghum liquor-making process. The oxidation capability of peroxymonosulphate arises from potassium peroxymonosulphate high redox potential, which is +1.81 V [13]. The kinetics of oxidation of cinnamyl alcohol by N-chloro-p-toluene sulphonamide (Chloramine-T) in an aqueous acid medium has been studied [14]. The reaction of ruthenium (III) chloride catalyzed oxidation of cinnamyl alcohol by thallium (III) has been studied in acid perchlorate medium [15]. The kinetic study of ruthenium (III) chloride catalyzed oxidation of paracetamol by *N*-chloro-*p*-toluene sulfonamide (chloramine-T) in the alkaline medium has been performed [16]. Chloramine-T (CAT), the sodium salt of N-chloro-p-toluenesulfonamide, is a low-cost mild oxidizing agent with a wide range of uses [17]. The activation parameters of the rate-determining steps were computed and the thermodynamic parameters were also calculated [18]. To further support our proposed mechanism, density functional theory (DFT) computations at M06/6-311*G show that activation energy barriers predict the same reactivity trend as shown by the kinetic experiments [19]. The ruthenium (III) catalysed redox reaction of paracetamol with hexacyanoferrate (III) in an acidic medium has been investigated [20]. It is very cleared from above literature survey that different group of researchers worked on of chloramphenicol by ionic oxidants in different media but no one worked on kinetic and thermodynamic investigation of oxidation of Chloramphenicol by metallic and nonmetallic ionic oxidants in aqueous conditions. Hence, the present study was undertaken.

2 Methodology

2.1 Chemicals

All the chemicals were analytical reagent quality, and Millipore water was used throughout the analysis. To prepare the chloramphenicol (Sisco research laboratories Pvt Ltd.) solution, known amounts of the samples were dissolved in millipore water (Sisco Chem). The purity of the sample was confirmed using by melting point 150°C. Before using, chloramphenicol solutions were typically prepared from scratch. Ruthenium trichloride trihydrate (Loba Chemie Pvt Ltd.) dissolved in 0.50 mol dm^{-3} HCl to makeup the Ruthenium (III) chloride stoke solution. To maintain the ionic strength and alkalinity of the reactions at the required levels, NaOH (Fisher Scientific) and $NaClO_4$ (Sigma Aldrich) were used. Iodometric estimation of the unreacted oxidant at regular intervals throughout the reaction was used to calculate the oxidation rate. The product p-nitrobenzaldehyde has been determined by the observed melting point of 320°C of the yellow coloured 2-4 dinitrophenylhydrazone derivative of p-nitrobenzaldehyde.

2.1.1. Solutions used

All the required stock and standard solution were made in double-distilled water (DDW). The chloramphenicol (SISCO Research Laboratories Pvt. Ltd.) is used as supplied without any purification; purity of chloramphenicol (CAP) is identified by melting point measurement 150 degree centigrade. Peroxymonosulfate [PMS] = 1.0×10^{-2} M, stock is prepared by weighing exact amount of solid and dissolving in DDW to makeup volume in volumetric flask, as like CAP stock solution is made of [CAP]= 1.0×10^{-2} M, [NaOH]= 1.0×10^{-2} M, [$RuCl_3$] = 1×10^{-3} M, [$Hg(OAc)_2$] = 3.33×10^{-2} M, [KCl]= 1×10^{-2} M, and

$[NaClO_4]$ =1×04 M. The aqueous solution of chloramphenicol (CAP), PMS and catalyst were kept in glass vessel that have been covered with black film on the outside, and the solution's stability is increased as decomposition is eliminated by diffused photoluminescence. Additionally, aqueous solution of CAP, PMS and catalyst Ru(III) were stored in a refrigerator at approximately 5°C. But a new chloramphenicol solution was always used. Stock of titrant hypo solution [Hypo]= 0.02 M (Approximate), is made in DDW and standardized by standard copper sulphate $[CuSO_4]$ = 0.02 M, solution by titrating an aliquot of the copper sulphate solution in the presence of KI, against hypo, the solution was standardized iodometrically. Using starch as an indicator with a sharp endpoint, the released iodine was titrated against a hypo solution. The PMS is also standardized by using hypo iodometrically. The NaOH stock solution is made by standardizing solution by standard oxalic acid by titration method using phenolphthalein indicator.

2.1.2. Scientific instruments

Titrimetric analysis is the best technique even today despite the advancement of new techniques but also UV-Visible spectrophotometer is also employed for this kinetic study. For determination of pH of the reaction mixture with maximum uncertainty 0.01 units in pH, digital pH meter is to be employed. Insulated water bath with an electronic circuit is used for the temperature measurements of the reaction, and heat oven for the sterilization of glass wares, were tools used in study.

2.1.3. Process

Unless otherwise stated, glass-stoppered Erlenmeyer flasks containing chloramphenicol, KCl, NaOH, and other ingredients aside from PMS were submerged in a circulating thermostated water bath at 35°C ± 0.3°C. To start the reaction, the temperature-pre-equilibrated PMS solution was added to the initial reaction mixture. When half of the pipette's solution was added to the reaction mixture, the initiation time was recorded. After giving the reaction mixture a good shake, an aliquot (5 cm^3) was taken at different intervals and added to a 10% KI solution. Using starch as an indicator, the free I_2 was titrated against a standard hypo solution. Under pseudo-first-order conditions ([CAP]) = ([PMS]), the reaction was studied. To find out the temperature effect on reaction rate we applied a temperature range from 303 to 328 K and same way, all the chemical reactions are studied by using an iodometric titration method.

3 Results and Discussion

3.1 Effect of Temperature

The effect of temperature was studied using two essential tools in chemical kinetics, the Arrhenius plot (Figure 1) and the Eyring plot (Figure 2).

$$k = Ae^{-\frac{Ea}{RT}}$$

The Eyring equation is derived from the transition state theory of chemical kinetics.

$$\ln\frac{k}{T} = \frac{-\Delta H^{\#}}{R}\frac{1}{T} + \ln\left(\frac{k_B}{h}\right) + \frac{\Delta S^{\#}}{R}$$

This leads to an Eyring plot of ln(k/T) versus 1/T, where the slope and intercept is used to yield the activation enthalpy $\Delta H^{\#}$ and the activation entropy $\Delta S^{\#}$, respectively. Table 1, 2 and 3 comprises all the experimental results for Ru(III)-catalyzed Chloramphenicol's degradation by peroxymonosulfate.

[PMS] = 1.0×10^{-3} M, [CAP]= 1.0×10^{-3} M, [NaOH]= 1.0×10^{-3} M, $[RuCl_3]$= 1×10^{-4} M, $[Hg(OAc)_2]$= 3.33×10^{-3} M, [KCl]= 1×10^{-3} M at 30° ± 0.3°C, 35° ± 0.3°C, 40° ± 0.3°C, 45° ± 0.3°C, 50° ± 0.3°C, 55° ± 0.3°C.

[PMS] = 1.0×10^{-3} M, [CAP]= 1.0×10^{-3} M, [NaOH]= 1.0×10^{-3} M, $[RuCl_3]$ = 1×10^{-4} M, $[Hg\,(OAc)_2]$ = 3.33×10^{-3} M, [KCl]= 1×10^{-3} M at 30° ± 0.3°C, 35° ± 0.3°C, 40° ± 0.3°C, 45° ± 0.3°C, 50° ± 0.3°C, 55° ± 0.3°C.

Table 1. Activation specifics in the Ruthenium (III) catalysed chloramphenicol's oxidation by peroxymonosulphate in basic medium.

$\Delta H^{\#}$ kJmol^{-1}	$\Delta S^{\#}$ JK^{-1}mol^{-1}	$\Delta G^{\#}$ kJmol^{-1}	$\Delta E^{\#}$ kJmol^{-1}	Ln A
27.683	-166.75	79.042	30.308	10.459

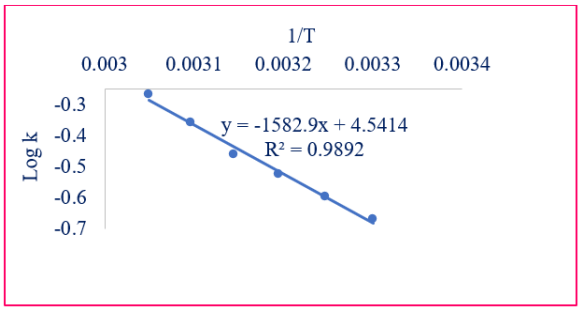

Fig 1. Arrhenius plot

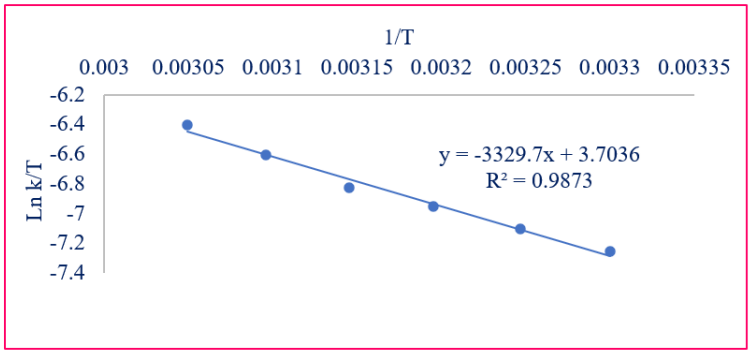

Fig 2. Eyring plot

3.2 Peroxymonosulphate (PMS) Dependence

The peroxymonosulphate (PMS) concentration was assorted from 1.0×10^{-3} mol L^{-1} to 4.0×10^{-3} mol L^{-1} at fixed concentration of other reaction ingredients viz. [CAP]= 1.0×10^{-3} M, [NaOH]= 1.0×10^{-3} M, [$RuCl_3$]= 1.0×10^{-4} M, [$Hg(OAc)_2$]= 3.33×10^{-3} M, [KCl]= 1×10^{-3} M at 35° ± 0.3°C. Initial rate plots are used to evaluate the rate constants. The rate constant values increase with increasing concentration of peroxymonosulphate indicating first order pertaining to PMS in the Ru(III) catalyzed reaction process (Figure 3).

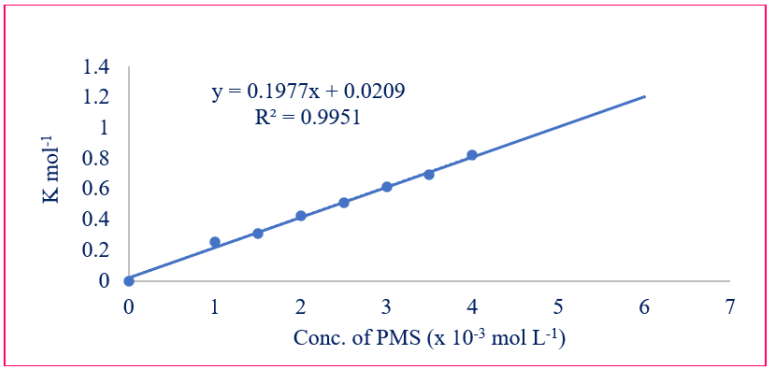

Fig 3. Peroxymonosulphate (PMS) variation plot

3.3 Effect of Chloramphenicol

The concentration of chloramphenicol was varied from 0.5×10^{-3} M to 4.0×10^{-3} M at fixed concentration of other reaction parameters viz; [PMS]= 1.0×10^{-3} M, [NaOH]= 1.0×10^{-3} M, [$RuCl_3$] = 1×10^{-4} M, [$Hg(OAc)_2$] = 3.33×10^{-3} M, [KCl]= 1×10^{-3} M at 35° ± 0.3°C (Figure 4). The initial rates are calculated, and a plot of initial rate versus chloramphenicol was made that yielded a variable order with chloramphenicol according to the following apparent rate equation.

$$-\frac{d[PMS]}{dt} = A + \frac{B[PMS][Ru(III)][CAP]}{1+C[CAP]}$$

Where,

A is apparent rate constant for the uncatalyzed reaction.

B is apparent rate constant for the catalysed reaction.

C is apparent equilibrium constant.

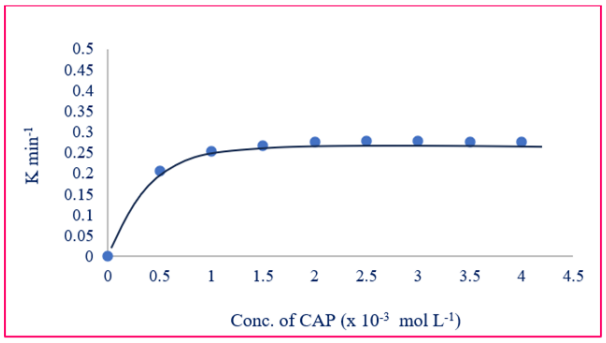

Fig 4. Chloramphenicol effect

3.4 Effect of Catalyst

During experiment, the concentration of the catalyst Ruthenium (III) was varied from 1.0×10^{-4} M to 4.0×10^{-4} M at fixed concentration of other reaction parameters viz; [PMS]= 1.0×10^{-3} M, [CAP]= 1.0×10^{-3} M, [NaOH]= 1.0×10^{-3} M, [$Hg(OAc)_2$] = 3.33×10^{-3} M, [KCl]= 1×10^{-3} M at 35° ± 0.3°C. A plot of initial rate against the concentration of Ruthenium (III) indicates catalysed and uncatalyzed path (Figure 5) and can be given by the following apparent rate equation.

$$\mathbf{k = D + E[Ru\,(III)\,]}$$

Where,

k is the rate constant indicating both catalysed and uncatalyzed pathway.

3.5 NaOH Variation

There has been variation in the sodium hydroxide content from 1×10^{-3} mol L^{-1} to 3.5×10^{-3} mol L^{-1} by employing fixed concentration of [PMS]= 1.0×10^{-3} M, [CAP]= 1.0×10^{-3} M, [$RuCl_3$] = 1×10^{-4} M, [$Hg(OAc)_2$] = 3.33×10^{-3} M, [KCl]= 1×10^{-3} M at 35° ± 0.3° C (Figure 6). The inverse effect is observed with increasing the sodium hydroxide concentration.

3.6 KCl Variation

Additionally, the impact of KCl concentration was studied from 1×10^{-3} mol L^{-1} to 4×10^{-3} mol L^{-1} at [PMS]= 1.0×10^{-3} M, [CAP]= 1.0×10^{-3} M, [NaOH]= 1.0×10^{-3} M, [$RuCl_3$] = 1×10^{-4} M, [$Hg(OAc)_2$] = 3.33×10^{-3} M at 35° ± 0.3° C. The rate shows a slight decrease pattern as shown in the Figure 7.

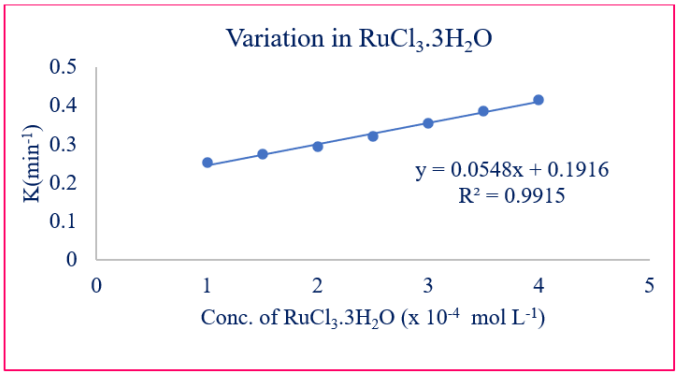

Fig 5. Catalyst Ruthenium (III) chloride trihydrate variation

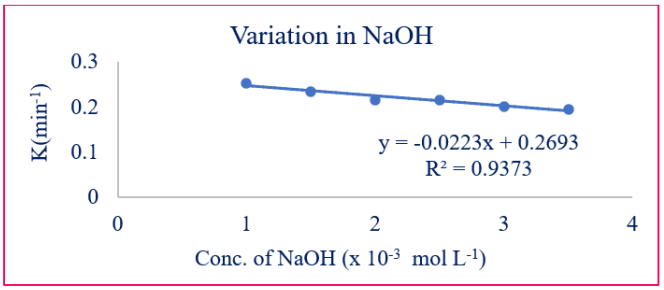

Fig 6. Sodium hydroxide variation

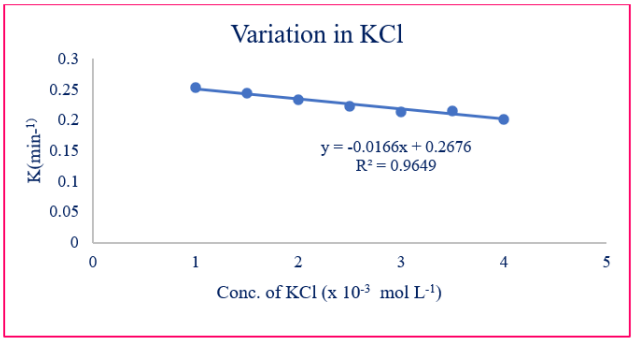

Fig 7. Effect of KCl variation

3.7 Effect of Ionic Strength

Sodium perchlorate was employed to study the effect of ionic strength. $NaClO_4$ has ranged from 0.2 mol L^{-1} to 1.2 mol L^{-1} at [PMS]= 1.0×10^{-3} M [CAP]= 1.0×10^{-3} M, [NaOH]= 1.0×10^{-3} M, [$RuCl_3$] = 1×10^{-4} M, [$Hg(OAc)_2$] = 3.33×10^{-3} M at 35° ± 0.3° C (Fig.8). The rate decreases with increasing the sodium perchlorate concentration, after a concentration that is approximate 1.0 M, a constant rate of reaction is observed (Figure 8).

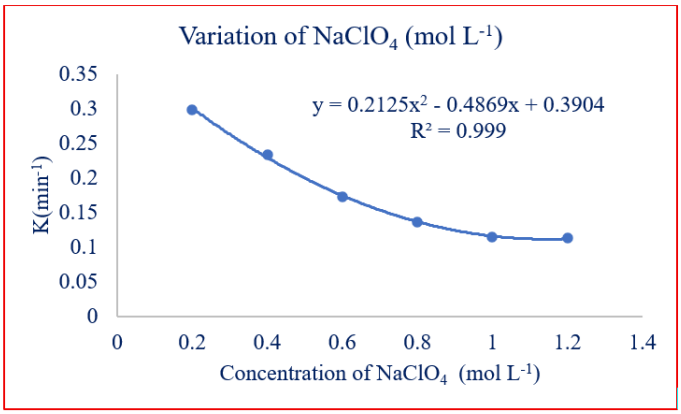

Fig 8. Effect of ionic strength

3.8 Discussion

The oxidation of chloramphenicol (CAP) by peroxymonosulphate (PMS) in aqueous basic medium is markedly accelerated by Ru(III) (ruthenium trichloride) and proceeds under pseudo-first-order conditions with respect to PMS. The observed pseudo-first-order rate constants increase proportionally with PMS, demonstrating first-order dependence on oxidant concentration. Variation of Ru (III) concentration produces a linear increase in rate constant, while extrapolation indicates a finite intercept, consistent with the coexistence of a slower uncatalyzed CAP–PMS reaction pathway alongside the Ru(III)-catalysed route. In contrast, changing chloramphenicol [CAP] produces only a small change in rate constant followed by an essentially concentration-independent region, indicating that chloramphenicol is not involved in the rate-determining step under the employed conditions and that the catalytic cycle is limited by oxidant activation rather than substrate availability. Increasing [OH^-] decreases rate constant, evidencing hydroxide inhibition that can be rationalized by PMS speciation (conversion of reactive HSO_5^- to less reactive SO_5^{2-}) and/or formation of less reactive hydroxo-Ru(III) species at higher alkalinity. Added electrolytes (KCl) also retard the reaction, and a pronounced decrease in rate constant with increasing $NaClO_4$ (ionic strength) further supports an inverse ionic-strength effect; this behaviour is diagnostic of an ionic rate-determining step in which electrostatic factors control the approach of reactants forming the activated complex. Collectively, these kinetic features support a mechanism involving rapid pre-equilibria (PMS speciation and Ru(III) hydroxo/association equilibria) followed by rate-determining activation of PMS by a catalytically competent Ru(III) species, with subsequent fast oxidation of CAP by a high-valent ruthenium intermediate and regeneration of Ru(III). All outcomes that were observed are provided in Table 1- 3 and Figure 1- 8.

$$HSO_5^- + OH^- \overset{K_b}{\rightleftharpoons} SO_5^{2-} + H_2O$$

$$Ru(III) + CAP \overset{K_s}{\rightleftharpoons} [Ru(III) - CAP]$$

If the reactive oxidant towards Ru (III) is HSO_5^- than

$$[HSO_5^-] = \frac{[PMS]}{1 + K_b[OH^-]}$$

$$Ru(III) + OH^- \overset{K_{OH}}{\rightleftharpoons} [Ru^{(III)}OH]$$

$$Ru(III) + HSO_5^- \overset{k_1}{\rightarrow} Ru(V) + SO_4^{2-} + H_2O$$

$$Ru(V) + CAP \overset{fast}{\rightarrow} Product + Ru(III)$$

$$CAP + PMS \overset{k_2}{\rightarrow} Product(UncatalysedPath)$$

$$Rate = \frac{-d[PMS]}{dt} = k_{obs}[PMS]$$

$$k_{obs} = k_2[CAP] + \frac{k_1[Ru(III)]}{(1 + K_b[OH^-])(1 + K_{OH}[OH^-]) + K_s[CAP]}$$

In addition, density functional theory (DFT) calculations were performed to characterize the electronic structure and optimized geometry of chloramphenicol, enabling correlation of computed descriptors (e.g., charge distribution, frontier orbital characteristics, and reactive-site localization) with the experimentally observed reactivity and product formation. The combined kinetic–thermodynamic analysis and DFT modeling therefore offer a coherent experimental–computational description of the Ru(III)–PMS oxidation pathway in alkaline medium.

3.9 Density Functional Theory (DFT)- calculations for Chloramphenicol

Density functional Theory (DFT) calculations are studied through 3D optimized structure 1, Ball and stick 3-D optimized molecular structure 2 and molecular electrostatic potential structure 3.

CAP- Energy Gap (ΔE = LUMO - HOMO) 4.65 eV

Property	Value
Homo Energy	**-5.92eV**
Lumo Energy	**-2.04eV**
HOMO- LUMO Gap	**3.88eV**

Geometry optimizations and frontier molecular orbital (FMO) energies were acquired at the M06-2X/6-31+G(d,p) level in the gaseous phase. The resultant HOMO and LUMO energies were employed for qualitative analysis of electronic softness/hardness and charge-transfer tendency among $RuCl_3$, chloramphenicol (CAP), and peroxomonosulphate (PMS).

At the M06-2X/6-31+G(d,p) level (gas phase), $RuCl_3$ exhibits the highest HOMO energy (−5.92 eV) and the smallest HOMO–LUMO gap (3.88 eV), signifying relatively enhanced electronic softness and propensity for charge redistribution. Chloramphenicol demonstrates an intermediate energy gap (4.65 eV; HOMO −6.98 eV; LUMO −2.33 eV), while PMS reveals the most stable HOMO (−7.85 eV) and the biggest energy gap (5.40 eV; LUMO −2.45 eV), indicative of a "harder" oxidant that is less susceptible to spontaneous charge rearrangement. The arrangement of gaps (PMS > CAP > $RuCl_3$) collectively endorses a mechanistic framework wherein Ru(III) acts as the electronically labile mediator that enables PMS activation (the turnover-limiting step), succeeded by the rapid oxidation of CAP by the activated oxidizing equivalent.

Table 2. Effect of varying oxidant PMS, chloramphenicol, Ru(III), NaOH and $Hg(OAc)_2$ (3.33×10^{-3}) M concentrations on the reaction rate at 308 K in aqueous basic medium

[PMS] $\times 10^{-3}$/ mol dm^{-3}	[CAP] ($\times 10^{-3}$)/ mol dm^{-3}	[Ru] $\times 10^{-4}$/ mol dm^{-3}	[OH^-] $\times 10^{-3}$/ mol dm^{-3}	KCl $\times 10^{-3}$/ mol dm^{-3}	K_C /min^{-1}
1.00	1.00	1.00	1.00	1.00	0.2533
1.00	1.50	1.00	1.00	1.00	0.2668
1.00	2.00	1.00	1.00	1.00	0.2762
1.00	2.50	1.00	1.00	1.00	0.2784
1.00	3.00	1.00	1.00	1.00	0.2796
1.00	3.50	1.00	1.00	1.00	0.2754
1.00	4.00	1.00	1.00	1.00	0.2762
1.00	1.00	1.00	1.00	1.00	0.2533
1.50	1.00	1.00	1.00	1.00	0.3087
2.00	1.00	1.00	1.00	1.00	0.4252
2.50	1.00	1.00	1.00	1.00	0.5124
3.00	1.00	1.00	1.00	1.00	0.6125
3.50	1.00	1.00	1.00	1.00	0.6914
4.00	1.00	1.00	1.00	1.00	0.8234
1.00	1.00	1.00	1.00	1.00	0.2533
1.00	1.00	1.50	1.00	1.00	0.2754
1.00	1.00	2.00	1.00	1.00	0.2941
1.00	1.00	2.50	1.00	1.00	0.3212
1.00	1.00	3.00	1.00	1.00	0.3549
1.00	1.00	3.50	1.00	1.00	0.3854
1.00	1.00	4.00	1.00	1.00	0.4152
1.00	1.00	1.00	1.00	1.00	0.2533
1.00	1.00	1.00	1.50	1.00	0.2345
1.00	1.00	1.00	2.00	1.00	0.2156
1.00	1.00	1.00	2.50	1.00	0.2151
1.00	1.00	1.00	3.00	1.00	0.2012
1.00	1.00	1.00	3.50	1.00	0.1954
1.00	1.00	1.00	1.00	1.00	0.2533
1.00	1.00	1.00	1.00	1.50	0.2435
1.00	1.00	1.00	1.00	2.00	0.2331
1.00	1.00	1.00	1.00	2.50	0.2231
1.00	1.00	1.00	1.00	3.00	0.2135
1.00	1.00	1.00	1.00	3.50	0.2154
1.00	1.00	1.00	1.00	4.00	0.2012

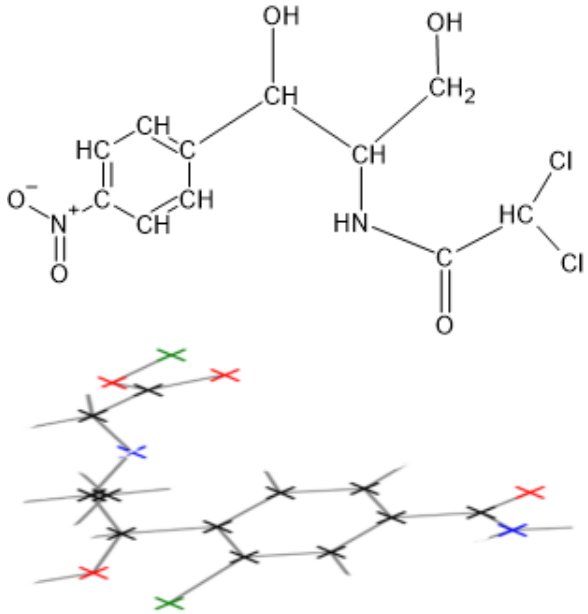

Fig 9. Chloramphenicol (CAP)- 3D Optimised structure

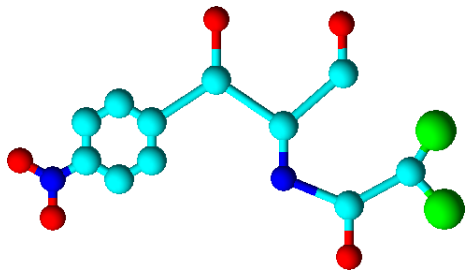

Fig 10. Ball and Stick 3-D optimized molecular Structure of Chloramphenicol

Table 3. Effect of ionic strength on the reaction rate at 308 K between CAP and PMS catalysed by Ruthenium trichloride in aqueous basic medium

$[NaClO_4]$ / mol dm^{-3}	$[PMS]\times10^{-3}$/ mol dm^{-3}	$[CAP]\times10^{-3}$/ mol dm^{-3}	$[Ru]\times10^{-4}$/ mol dm^{-3}	$[OH^-]\times10^{-3}$/ mol dm^{-3}	$KCl\times10^{-3}$/ mol dm^{-3}	K_C/min^{-1}
0.2	1	1	1	1	1	0.2994
0.4	1	1	1	1	1	0.2341
0.6	1	1	1	1	1	0.1735
0.8	1	1	1	1	1	0.1359
1	1	1	1	1	1	0.1152
1.2	1	1	1	1	1	0.1135

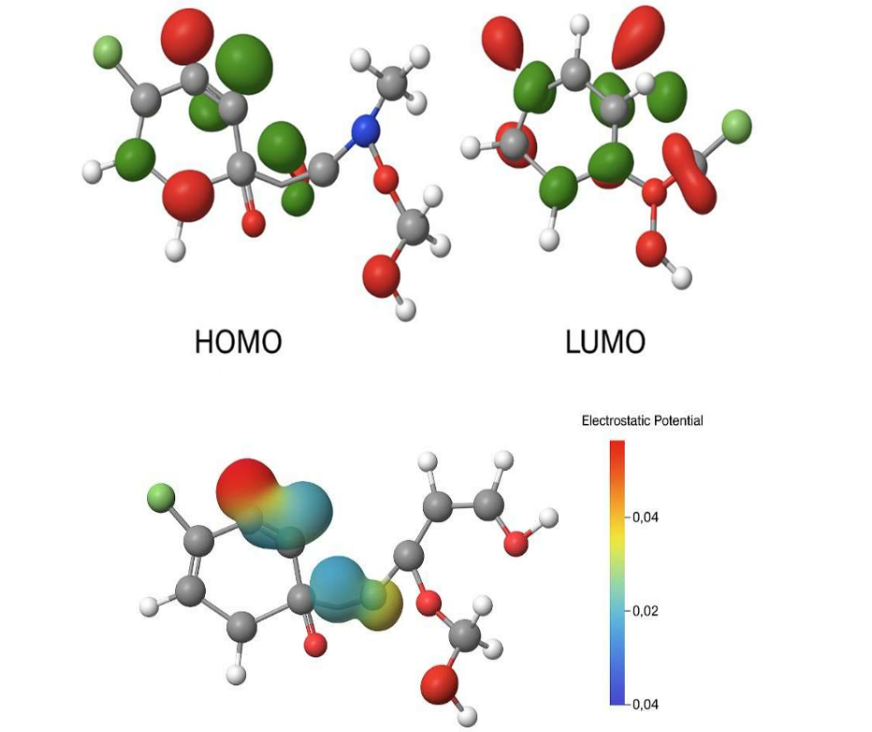

Fig 11. MEP- Molecular Electrostatic Potential of the Chloramphenicol

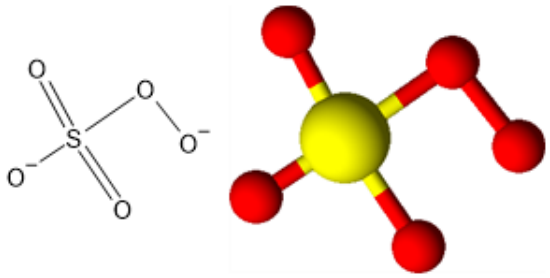

Fig 12. Density Functional theory – for the Peroxomonosulphate

4 Conclusion

The Ru(III)-catalysed oxidation of chloramphenicol (CAP) by peroxomonosulphate (PMS) in aqueous basic medium proceeds efficiently under pseudo-first-order conditions with respect to PMS. The kinetic data show first-order dependence on PMS and a linear dependence on Ru(III) with a finite intercept, confirming the coexistence of parallel uncatalyzed and catalysed reaction pathways. Variation of CAP produces only a weak effect followed by an approximately concentration-independent region, indicating that substrate oxidation occurs in a fast step after formation of an active oxidizing intermediate and that the overall rate is governed primarily by oxidant activation. The reaction is retarded by hydroxide ions, attributable to PMS speciation (depletion of the more reactive HSO_5^- form) and/or formation of less reactive hydroxo–Ru(III) species in stronger base. Added electrolytes (KCl) and ionic-strength variation using $NaClO_4$ significantly decrease the rate, establishing an inverse ionic-strength effect and supporting an ionic rate-determining step involving Ru(III)–PMS interaction. Collectively, these findings support a mechanism comprising rapid pre-equilibria (PMS speciation and Ru(III) hydroxo/association equilibria) followed by rate-determining activation of PMS by a catalytically competent Ru(III) species to generate a high-valent ruthenium

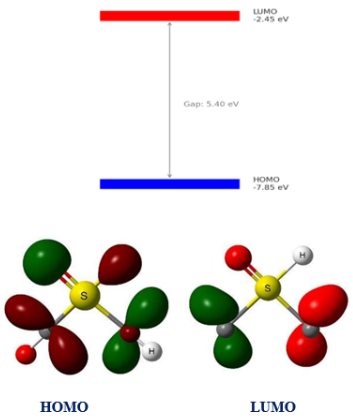

Fig 13. HOMO–LUMO Summary: HOMO-LUMO ENERGY LEVEL DIAGRAM FOR PEROXOMOMOSULPHATE

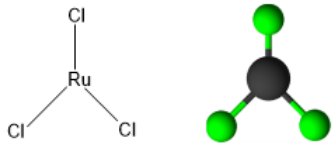

Fig 14. Density Functional Theory for the Ruthenium trichloride

oxidant, which rapidly oxidizes CAP with regeneration of Ru(III). The derived composite rate law satisfactorily rationalizes the observed dependences on PMS, Ru(III), CAP, OH^-, and ionic strength.

Thermodynamic functions and Eyring activation values were ascertained for the rate-limiting step, offering an energetic basis for the suggested catalytic mechanism. Furthermore, DFT calculations conducted to elucidate the electronic structure of the reactants and the hierarchy (PMS > CAP > $RuCl_3$) corroborate the experimental finding that Ru(III) acts as the redox mediator, promoting PMS activation, which is succeeded by the swift oxidation of CAP to products (including p-nitrobenzaldehyde) alongside the regeneration of the catalyst.

This work introduces a mechanistically resolved kinetic framework for the Ru(III)-catalysed oxidation of chloramphenicol by peroxymonosulphate in alkaline solution. Unlike many substrate-focused oxidation studies, the kinetic signatures here identify oxidant activation as the dominant control element: These results support a catalytic cycle in which a catalytically competent Ru(III) species activates peroxymonosulphate to a higher-valent ruthenium oxidant that rapidly converts chloramphenicol to products (including p-nitrobenzaldehyde), and they enable a composite rate law that explicitly couples oxidant speciation, catalyst speciation, and ionic-strength control—features that are rarely quantified concurrently in homogeneous organic oxidation kinetics.

5 ACKNOWLEDGEMENTS

Authors are thankful to the Head, Department of Chemistry, Jai Narain Vyas University, Jodhpur, Rajasthan, INDIA for research laboratory facilities and Dilip Kumar (one of the authors) is thankful to Dr. Anita Meena, for scientific analysis during research work.

6 CRediT authorship contribution statement

Dilip Kumar: Methodology, Investigation, Writing – original draft, Writing – review & editing, Formal analysis. Anita Meena: Methodology, Resources, Data curation. Anita Meena: Conceptualization, Supervision, Resources. Dilip Kumar: Formal analysis. Anita Meena: Supervision.

Conflicts of interests: There are no conflicts to declare.

Competing financial interests: The authors declare that they have no known competing financial interests or personal relationships that could have appeared to influence the work reported in this manuscript.

Data Availability Statement: All the data have been incorporated in the manuscript.

References

1) Ranucci E, Alongi J. Thermal Decomposition of Cellulosic Materials: Insights into Mechanisms and Product Evolution. *Polymer Degradation and Stability*. 2025;p. 111629. 10.1016/j.polymdegradstab.2025.111629.
2) Nagarajan D. .
3) Kaur K, Akhtar T, Singh G, Kaur N, Singh N. Rapid detection and visible light driven photocatalytic degradation of chloramphenicol in aqueous medium using a $CoAl_2O_4$/Rgo nanocomposite. *New Journal of Chemistry*. 2025;49:4668–4681. 10.1039/D4NJ05369.
4) Singh S. Osmium (VIII)-catalyzed oxidative degradation of paracetamol by chloramine-T in an aqueous alkaline medium: computational screening and mechanistic pathways. *RSC Advances*. 2025. 10.1039/D5RA03805G.
5) Arpitha MK, Vidyashree KM, Sonakshi HS, Jayadevappa HP. A comparative kinetic study of uncatalyzed and Ce(IV) catalyzed cetrizine dihydrochloride oxidation in aqueous acid medium by chloramine-T. *Asian Journal of Chemistry*. 2024;36(4):955–962. 10.14233/ajchem.2024.31305.
6) Byadagi K, Meti M, Nandibewoor S, Chimatadar S. Catalytic Activity of Palladium (II) and Osmium (VIII) on the Oxidation of Chloramphenicol by Copper (III) Periodate Complex in Aqueous Alkaline Medium: A Comparative Kinetic and Mechanistic Approach. *Industrial & Engineering Chemistry Research*. 2013;52(26):9011–9020. 10.1021/ie400097n.
7) Zhang Y, Shao Y, Gao N, Gao Y, Chu W, Li S, et al. Kinetics and by-products formation of chloramphenicol (CAP) using chlorination and photocatalytic oxidation. *Chemical Engineering Journal*. 2018;333:85–91. 10.1016/j.cej.2017.09.094.
8) Zhou JH, Chen KB, Hong QK, Zeng FC, Wang HY. Degradation of chloramphenicol by potassium ferrate (VI) oxidation: kinetics and products. *Environmental Science and Pollution Research*. 2017;24(11):10166–10171. 10.1007/s11356-017-8656-7.
9) Tan C, Fu D, Gao N, Qin Q, Xu Y, Xiang H. Kinetic degradation of chloramphenicol in water by UV/persulfate system. *Journal of Photochemistry and Photobiology A: Chemistry*. 2017;332:406–412. 10.1016/j.jphotochem.2016.09.021.
10) Cheng F, Zhou P, Liu Y, Huo X, Zhang J, Yuan Y, et al. Graphene oxide mediated Fe (III) reduction for enhancing Fe (III)/H2O2 Fenton and photo-Fenton oxidation toward chloramphenicol degradation. *Science of The Total Environment*. 2021;797:149097. 10.1016/j.scitotenv.2021.149097.
11) Shmychkova O, Zahorulko S, Luk'yanenko T, Velichenko A. Electrochemical oxidation of chloramphenicol with lead dioxide–surfactant composites. *Water Environment Research*. 2021;93(11):2716–2726. 10.1002/wer.1628.
12) Yen SW, Chen WH, Chang JS, Eng CF, Naqvi SR, Show PL. Torrefaction thermogravimetric analysis and kinetics of sorghum distilled residue for sustainable fuel production. *Sustainability*. 2021;13(8):4246. 10.3390/su13084246.
13) Sharma P, Sailani R, Meena A, Khandelwal CL. Oxidation of crotyl alcohol by N-chloro-4-methylbenzene sulphonamide in acidic medium and in alkaline media in the presence of Os(VIII) catalyst—a kinetic pathway. *Turkish Journal of Chemistry*. 2020;44(4):950–970. 10.3906/kim-2003-67.
14) Meena A. The Kinetics and Mechanism of Oxidation of Cinnamyl Alcohol by N-Chloro p-toluene Sulphonamide (Chloramine-T) in Acid Perchlorate Medium. *Indian Journal of Chemistry (IJC)*. 2023;62(8):803–807. 10.56042/ijc.v62i8.87.
15) Meena A, Bhasin M, Sharma P, et al. Kinetics and Mechanism of Ruthenium(III) Chloride Catalyzed Oxidation of Cinnamyl Alcohol by Thallium(III) in Acid Perchlorate Medium. *Russian Journal of Physical Chemistry*. 2021;95:2553–2557. 10.1134/S0036024421130148.
16) Pareek D, Rolaniya A, Bhasin M, Sailani R. Ruthenium (III) catalyzed oxidation of paracetamol by chloramine-T in aqueous alkaline medium–A kinetic and mechanistic pathway. *International Journal of Chemical Kinetics*. 2023;55(1):39–48. 10.1002/kin.21613.
17) Nayak YN, Gaonkar SL, Saleh EAM, Dawsari AMA, Husain K, Hassan I. Chloramine-T (N-chloro-p-toluenesulfonamide sodium salt), a versatile reagent in organic synthesis and analytical chemistry: An up to date review. *Journal of Saudi Chemical Society*. 2022;26(2):101416. 10.1016/j.jscs.2021.101416.
18) Srivastava A, Kumar V, Verma A, Devi P, Singh A. Kinetic, Mechanistic, and Quantum Chemical Study of Osmium (VIII)-Catalyzed Bromination of Paracetamol by Acidic N-Bromosuccinimide (Iodometric Titration). *Russian Journal of Organic Chemistry*. 2024;60(1):101–114. 10.1134/S1070428024010147.
19) Pareek D, Rolaniya A, Yadav A, Sailani R. Oxidative Degradation of Paracetamol by N-Bromo Succinimide in Presence of Mercuric Acetate–A Computational Screening and Mechanistic Pathway. *Russian Journal of Physical Chemistry A*. 2024;98(4):552–559. 10.1134/S0036024424040058.
20) Rolaniya A, Yadav A, Jain P, Sailani R. Experimental and Computational Kinetic Assessment of Ruthenium (III) Catalyzed Oxidation of Paracetamol by Hexacyanoferrate (III): A Mechanistic Pathway. *ChemistrySelect*. 2024;9(2):e202303734. 10.1002/slct.202303734.